Science & Technology Development Journal 2025, 28(2):3770-3778

Open Access Full Text Article

Research Article

Ab initio Chemical Kinetics of the Isobutene + SiH_3 Reaction

Uyen N-P. Tran[1,2], Loc T. Nguyen[1,2], Khoi M. Le[1,2], Tam V.-T. Mai[1,3], Lam K. Huynh[1,2,*]

ABSTRACT

The detailed kinetic mechanism between isobutene and SiH_3 radicals was investigated theoretically using the composite electronic structure method CBS-QB3 in conjugated with the Rice–Ramsperger–Kassel–Marcus based master equation (RRKM-ME) rate modeling. The study reveals that the title reaction proceeds through two primary pathways: (*i*) addition of SiH_3 to the double bond and (*ii*) H-abstraction by SiH_3, leading to various products. The addition pathway forms two primary products, **P3** and **P4**. The H-abstraction pathway results in two product channels, **P1** + SiH_4 and **P2** + SiH_4. Among these, the adduct **P3** is identified as the most thermodynamically and kinetically favorable intermediate at $T < 900$ K. However, at $T > 900$ K, **P1** and **P4** gain prominence. Pressure effect analysis (at $P = 7.6$ - 76000 Torr) shows that pressure has no significant influence on the reaction mechanism. The branching ratio calculation confirms **P3**'s dominance below 900 K, peaking at 99.8% at 200 K. At 2000 K, **P1** and **P4** dominate with ratios of 61.9% and 30.5%, respectively. In our search for a suitable method to calculate thermodynamic properties, we found that the atomization scheme at the CBS-QB3 level is suitable for S^{298K} and $C_p{}^{298K}$, while the isodesmic reaction scheme is recommended for $\triangle_f H^{298K}$ calculations. The calculated geometrical parameters, thermodynamic properties, and kinetic data align with existing/related literature for selected species, indicating the reliability of the study. These findings provide further mechanistic insights as well as reliable information for detailed kinetic modeling of silicon chemical vapor deposition (CVD) processes, which are of significant technological importance.

Key words: isobutene, SiH3, reaction mechanism, CBS-QB3, chemical vapor deposition (CVD)

[1]*Vietnam National University Ho Chi Minh City, Vietnam*

[2]*International University, Quarter 6, Linh Trung Ward, Thu Duc City, Ho Chi Minh City, Vietnam*

[3]*University of Science, 227 Nguyen Van Cu, Ward 4, District 5, Ho Chi Minh City, Vietnam*

Correspondence

Lam K. Huynh, Vietnam National University Ho Chi Minh City, Vietnam

International University, Quarter 6, Linh Trung Ward, Thu Duc City, Ho Chi Minh City, Vietnam

Email: hklam@hcmiu.edu.vn

History

- Received: 30-12-2024
- Accepted: 21-04-2025
- Published Online: 21-06-2025

DOI :

https://doi.org/10.32508/stdj.v28i2.4398

INTRODUCTION

Silicon carbide (SiC) stands out as a semiconductor due to its ability to operate under higher temperatures and currents, offering distinct advantages over silicon-based materials like silicon dioxide (SiO_2) or silicon nitride (Si_3N_4)[1,2,3]. The production of silicon carbide typically involves methods such as chemical vapor deposition (CVD) or plasma-enhanced chemical vapor deposition (PECVD). These methods use silicon and carbon precursors, typically silane (SiH_4) and hydrocarbons, to deposit the thin film of the material through a controlled gas-phase combustion process[4]. During deposition, silane decomposes into various reactive mono-silicon hydride radicals like SiH, SiH_2, and SiH_3. Among these, silyl (SiH_3) radicals are believed to have the highest contribution, driving the hydrosilylation mechanism to form Si-C bonds[5,6]. The use of olefins as precursors further enhances the hydrosilylation reaction. Their double bonds significantly boost the chemical reactivity, enabling more efficient and precise film deposition. This enhancement underscores the importance of silyl radical addition to double bond as a key mechanism in olefin hydrosilylation[7]. To better understand and optimize this process, it is crucial to study how the reactivity of different alkenes affects their interaction with silyl radicals. Such insights are vital for improving the efficiency and quality of SiC film production.

In 1990, Loh *et al.*[8] experimentally reported the rate constant for C_3H_6 + SiH_3 reaction at ambient condition (e.g. $k(C_3H_6) = (2.4\pm0.3)\times10^{-13}$ cm^3/molecule/s), which is at least two orders of magnitude larger than that for the C_2H_4 + SiH_3 reaction (e.g. $k(C_2H_4) \leq (3.0\pm3.0)\times10^{-15}$ cm^3/molecule/s). They also studied the effect of pressure variation on the reactions, ranging from 2 to 9.5 Torr, and found that pressure had no effect. Later, in 1991, Loh *et al.*[9] studied the gas-phase pseudo-first order reaction between SiH_3 and C_3H_6 at room temperature and pressure 9.5 Torr and reported that the rate constant for C_3H_6 + SiH_3 reaction (e.g. $k(C_3H_6) = (1.5\pm0.5)\times10^{-14}$ cm^3/molecule/s) is lower than that of the previous study conducted in 1990 (e.g. $k(C_3H_6) = (2.4\pm0.3)\times10^{-13}$ cm^3/molecule/s). They also found that hydrogen abstraction pathways are exothermic and silyl addition is also presumably energetically allowed.

However, Bottoni *et al.*[10] conducted a study on the silyl-initiated oxidation with C_2H_4, and C_3H_6 in

Cite this article : Tran U N, Nguyen L T, Le K M, Mai T V, Huynh L K. **Ab initio Chemical Kinetics of the Isobutene + SiH_3 Reaction**. *Sci. Tech. Dev. J.* 2025; 28(2):3770-3778.

1997. The optimized geometries of all species related to the reaction mechanism of the two reactions are calculated at MP2/6-31G* level and QCISD(T)/6-311G** level, respectively. The calculated energy barrier in this study has rejected the common belief that alkyl substituent enhances the hydrogen abstraction pathway[11] and suggests that alkyl substituent activates olefin toward the silyl addition pathway in the gas phase. Additionally, Clarkin *et al.*[12] conducted thermochemistry and kinetic for C_2H_4 + SiH_3 addition reaction using UQCISD(T) method with aug-cc-pVTZ and aug-cc-pVDZ basis sets. The resulting activation energy and reaction enthalpy (e.g., E_a = 3.3 kcal/mol, and DH_{rxn} = -20.6 kcal/mol at 298 K) have pointed out the studies of Bottoni *et al.*[10] were insufficient for accurately determining activation energy. Liu *et al.*[13] also studied the addition mechanism for the C_3H_6 + SiH_3 reaction at the B3LYP/6-311++G(d,p) level and observed that the energy barrier of addition pathways is around 2.9 kcal/mol, which is relatively good in accordance with the previous research conducted by Bottoni *et al.*[10] . These studies have significantly advanced our comprehension of kinetic and thermodynamics in the hydrosilylation reaction of alkenes (e.g., ethene[8, 10, 12] and propene[8, 10, 13]). However, the specific influence of alkyl substituents on the relative contributions of silyl addition and hydrogen abstraction pathways contributions remains unclarified.

In this study, within the framework of investigating the effect of alkyl substituents on the reactivity of double bond in the hydrosilylation reaction, the reaction mechanism and kinetic behavior for the reaction of isobutene with silyl radicals are examined to see the effect of two methyl substituents at the same double-bond carbon on the activity. The reaction mechanism will be structured using electronic structure calculations, calculated at the CBS-QB3 level with hindered internal rotation (HIR) treatment at the B3LYP/CBSB7 level.

METHODOLOGY

The electronic structure calculations were performed using the GAUSSIAN 09 program[14]. Among the various correlated methods available, the CBS-QB3 composite method was chosen for its balance of accuracy and computational efficiency[15]. The geometries of all stationary points involved in the reaction, including reactants, products, intermediates, and transition states (TSs), were optimized using the B3LYP functional with the CBSB7 basis set[16, 17, 18, 19, 20]. Single-point energies at the CBS limit were obtained through a predefined extrapolation scheme that combines multiple basis sets and incorporates empirical corrections, specifically tailored to improve accuracy for small organic system[15]. This method has been successfully applied to study the thermodynamics and kinetics of similar and larger oxygenated systems. For example, it was used to investigate the decomposition of methyl-ester peroxyl radicals in the low-temperature oxidation of methyl butanoate[21]. In the case of complex reaction pathways, the correct transition state was confirmed by calculating the minimum energy paths (MEP) from the transition state to both the reactants and products using the intrinsic reaction coordinate (IRC) method[22, 23].

The standard heat of formation for isobutene involved was calculated using the atomization energy method, as described in reference[22, 24]. Within the framework of classical statistical mechanics, the entropies and isobaric heat capacities of the species were determined (detailed calculations can be found in the supplementary material of Duong *et al.*)[25, 26]. These calculations were carried out using the Multi-Species Multi-Channels (MSMC) code[27]. The stochastic[28, 29] RRKM-ME rate model[30] in the MSMC code[27,31], was used to determine the rate coefficients with a number of trials of 10^6 for the energy profile in Figure 1. Our calculations also included corrections for Eckart tunneling[32] and the HIR treatments.

We employed the single exponential energy transfer model with a temperature-dependent expression of $\langle\Delta E_{down}\rangle$ = 250.0 × $(T/298)^{0.8}$ cm^{-1} for N_2 bath gas[33]. Lennard-Jones parameters were ε/k = 82.0 K and = 3.74 Å for N_2 from Hippler *et al.*[34], while ε/k = 336 K and = 4.13 Å, based on carbonyl sulfide[35] , for the reactant complex and intermediate adducts. Density and sum of states were calculated using the Beyer–Swinehart algorithm[36] combined with external/hindered rotational modes via FFT[37] with a density-of-states energy bin size of 1 cm^{-1}. The pre-reactive van der Waals (vdW) complex entrance channel is barrierless. The initiation process was handled using the inverse Laplace transform (ILT) approach[38] yielding $k(E)$ and a temperature-independent HPL rate constant $k^{\infty}(T) = 4.0 \times 10^{-10}$ cm^3/molecule/s as suggested by Georgievskii et al.[39] for the hydroxylation due to limited information on the vdW rate formation in the hydrosilylation.

RESULTS AND DISCUSSION

As observed in the reaction of isobutene with OH radicals (cf. Figure 1), two distinct mechanisms are identified: (*i*) direct hydrogen abstraction from

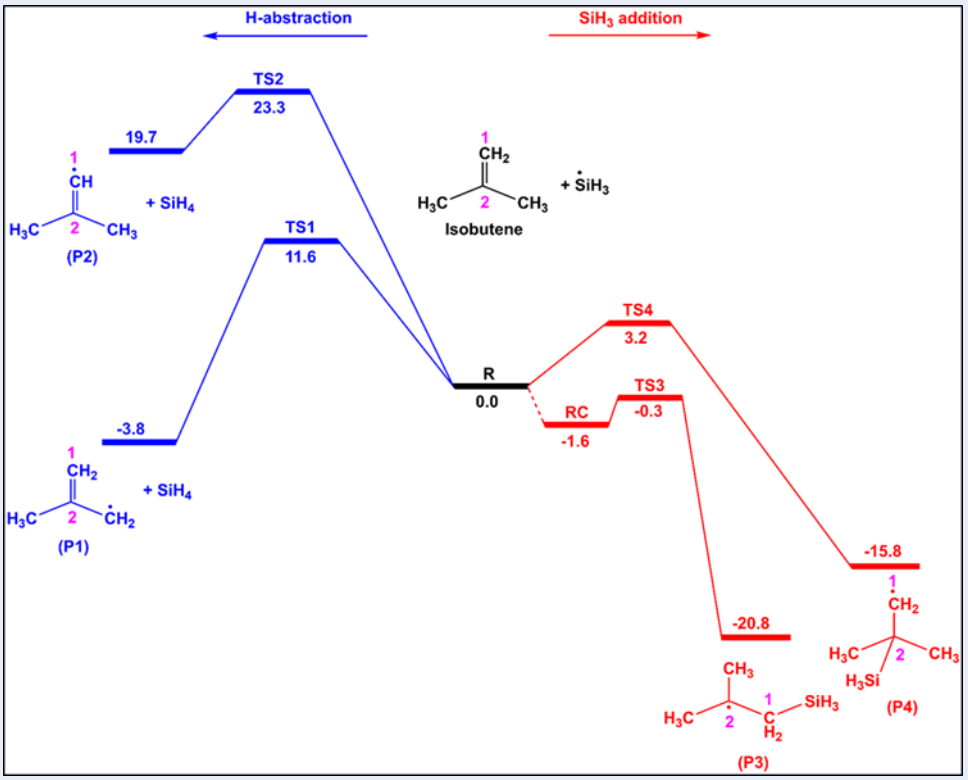

Figure 1: ZPE-corrected energy profile (0 K) for the isobutene + SiH_3 reaction. Units are in kcal/mol.

CH_2=C(CH_3)$_2$ by SiH_3 radicals and (*ii*) the addition of SiH_3 radicals to the C=C double bond of CH_2=C(CH_3)$_2$ (1).

(i) Abstraction channels: Similar to the reaction of isobutene with OH radicals, SiH_3 radicals can abstract a hydrogen atom from the -CH_3 and =CH_2 moieties of CH_2=C(CH_3)$_2$, which require overcoming barriers at **TS1** (11.6 kcal/mol) and TS2 (23.3 kcal/mol), respectively (1). The most favorable direct H-abstraction pathway via **TS1** requires approximately 11.6 kcal/mol more energy than the addition pathway via **TS3**. Consequently, due to the significant difference in barrier heights between the abstraction and addition processes, the H-abstraction channel is expected to have a minimal effect, particularly at low temperatures. Subsequently, the final products, **P1** and **P2**, are formed, with energies of -3.8 kcal/mol and 19.7 kcal/mol, respectively. The formation of **P1** is in agreement with Loh *et al.*[9] that H-abstraction product could be exothermic.

(ii) Addition channels: The SiH_3 radical can add to the C=C bond of CH_2=C(CH_3)$_2$, forming two distinct products, P3 and P4, which are located at -20.8 and -15.8 kcal/mol below the energy of the entrance channel, respectively. These intermediates are accessed via the transition states **TS3** and **TS4**. Notably, the transition state for SiH_3 addition to the C1 position exhibits a lower barrier height (-0.3 kcal/mol) compared to the addition at the C2 position (4.2 kcal/mol) (see Figure 1). Note that the optimized geometries for all species involved in the PES are depicted in Figure S1. To summarize, **P3** is the most thermodynamically and kinetically favorable adduct which agrees with the idea that OH-addition is important in the reaction of alkyl substituents with SiH_3 (10, 12, 13). However, at high temperatures (e.g., $T \geq$ 1000 K), direct H-abstraction may become significant due to the entropy effect at elevated temperatures[40]. Therefore, a detailed kinetic analysis is necessary to make more accurate predictions for this system, particularly across a wide range of *T*&*P* conditions.

Figure 2 depicts our comparison between three species, namely isobutene, SiH_3, and SiH_4, with available measurements/predictions (optimized isobutene from Tian *et al.*'s work (1), SiH_3 from Yamada *et al.*'s work[41], and SiH_4 from Kuchitsu *et al.*'s work[42]) in terms of geometries, bond lengths, and angles. The good agreement in geometries, bond lengths, and angles (i.e., within 1%) indicates the reliability of the

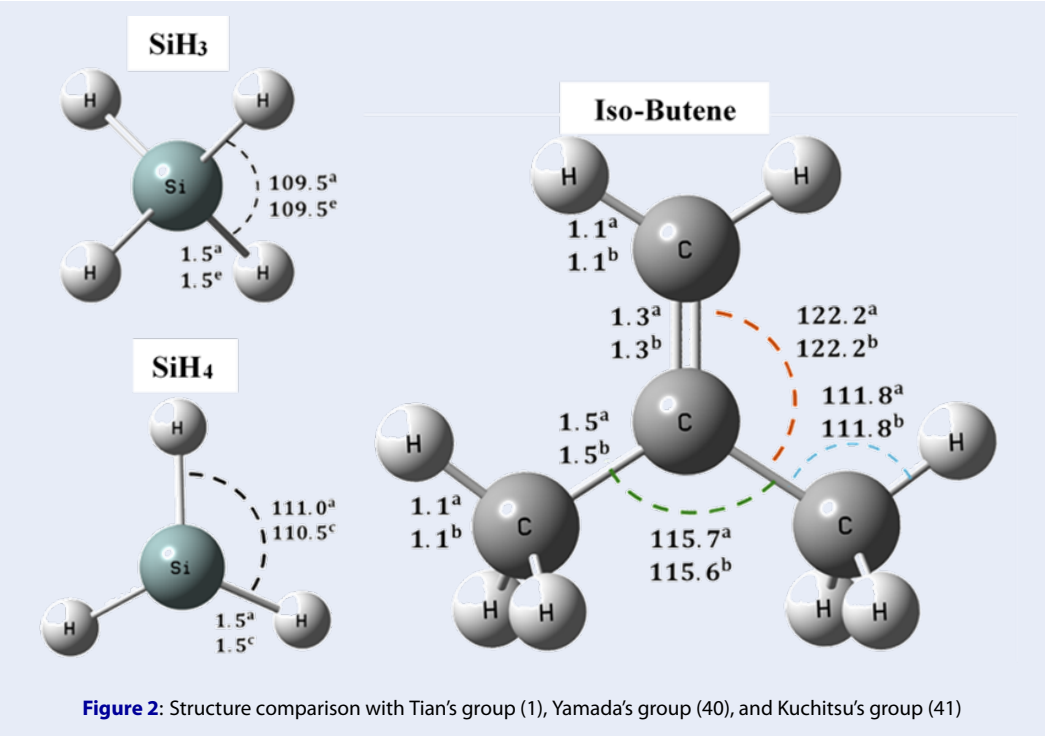

Figure 2: Structure comparison with Tian's group (1), Yamada's group (40), and Kuchitsu's group (41)

study. For more details on other species, please see the supplementary material.

Thermodynamic analyses

Table 1 compares thermodynamic data for isobutene, calculated using the CBS-QB3 method, with previously reported values. Two calculation schemes (i.e., atomization and isodesmic reaction) were employed. The atomization scheme at the CBS-QB3 level shows good agreement with the literature for S^{298K} and $C_p{}^{298K}$ (i.e., within 0.2 cal/mol/K), but discrepancies were observed for $\triangle_f H^{298K}$. To address this, we used an isodesmic reaction approach implemented in our in-house RGA4HoF code[43]. The code generated 3020 isodesmic reactions and estimated the average value. Detailed 3020 reactions are provided in the supplementary material file. The $\triangle_f H^{298K}$ values obtained from the isodesmic reaction scheme align well with the literature (i.e., within the reported uncertainty). In conclusion, the atomization scheme at the CBS-QB3 level is suitable for S^{298K} and $C_p{}^{298K}$, while the isodesmic reaction scheme is recommended for $\triangle_f H^{298K}$ calculations. Note that the comparison for other species was not carried out due to the limited literature data.

Kinetic analyses

Figure 3 presents the rate constant comparison with the uncertainty of the ILT approach for the formation of **RC**. The uncertainty assessment is necessary due to the differences in the nature of the interactions of the vdW complex in hydroxylation and hydrosilylation. Importantly, we found that the choice of the HPL rate has a minor effect at temperatures between 200 and 2000 K, resulting in a 1.0 to 1.7 times different total rate constant. This indicates that the assumption does not change the kinetic behavior of the hydrosilylation. Since there is no kinetic data available yet for this system, we presented the rate constants for the C_3H_6 + SiH_3 and C_2H_4 + SiH_3 systems. The upper limit is found to be comparable to the experiment of C_3H_6 + SiH_3 by Loh *et al.* (1990)[8] (1.7×10^{-13} vs. $(2.4\pm0.3)\times10^{-13}$ cm^3/molecule/s), while the lower limit is quite far-fetched compared to the experiment on C_3H_6 + SiH_3 by Loh *et al.* (1991)[9] (1.0×10^{-13} vs. $(1.5\pm0.5)\times10^{-14}$ cm^3/molecule/s) and C_2H_4 + SiH_3 by Loh *et al.* (1990)[8] (1.0×10^{-13} vs. $(3.0\pm3.0)\times10^{-14}$ cm^3/molecule/s). However, note that due to differences in the nature of the reactions and the possibility that the experiment on C_3H_6 + SiH_3 by Loh *et al.* (1990) may have been overdetermined due to the photolysis of C_3H_6, further experiments on the isobutene + OH reaction are needed

Table 1: Computed and literature thermochemical data at 298.15 K for isobutene.

Methodology	$\triangle_f H^{298K}$ (kcal/mol)	S^{298K} (cal/mol/K)	C_p^{298K} (cal/mol/K)
Atomization scheme at CBS-QB3	-1.81	70.31	20.85
Isodesmic reaction scheme at CBS-QB3 $(CH_3)_2C=CH_2$ + cyclo-pentane $\rightarrow CH_3CH=CH_2$ + cyclo-hexane (The best-matched reaction among 3020 reactions found)	-3.97	-	-
Literature data	-4.03 ± 0.38 [43] -4.28 ± 0.26 [44]	70.12 [45]	21.04 [46]

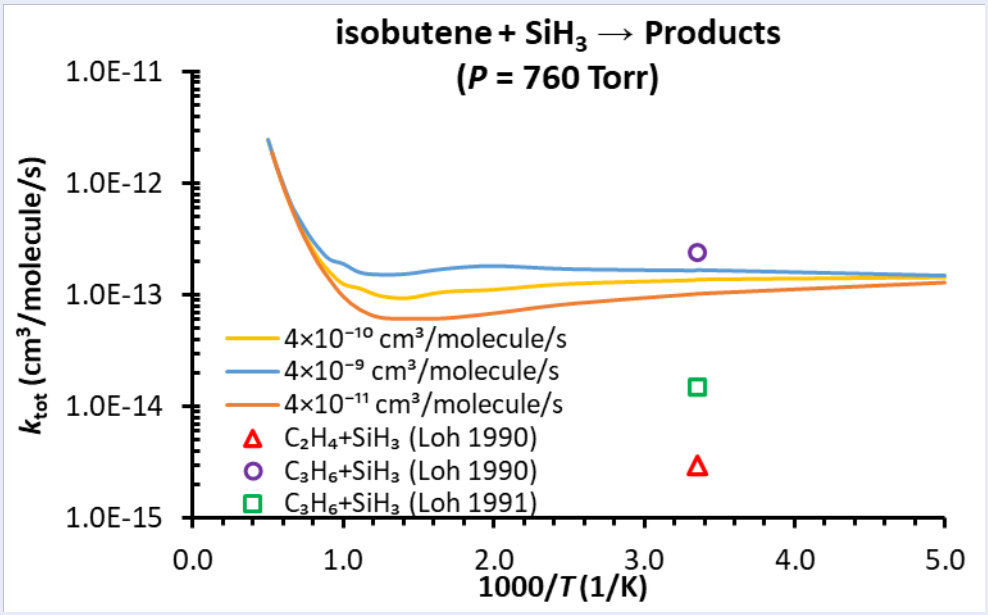

Figure 3: Rate constant comparison together with the uncertainty analysis of the ILT approach

for better understanding on the effect of the methyl groups on the activity.

We found that **P3** is dominant at temperatures below 900 K, with a maximum branching ratio of 99.8% at 200 K (cf Figure 4 and Table 2). At higher temperatures, **P1** and **P4** become dominant, with branching ratios reaching 61.9% and 30.5%, respectively, at 2000 K. This kinetic behavior agrees well with the predictions discussed in the energy profile analysis. Note that the decomposition of P3 might also be important at high temperatures.

We tested the pressure effect on the isobutene + SiH_3 reaction (cf. Figure 5) at P = 7.6 - 76000 Torr, inspired by the idea of Loh et al.[8] (1990) that alkyl substituents would exhibit no pressure effect in reactions with SiH_3. This was confirmed in our study (cf. Figure 5), as we also found no pressure effect on the isobutene + SiH_3 reaction.

CONCLUSIONS

The kinetic mechanism of the reaction between isobutene and SiH_3 radicals was investigated theoretically using the composite electronic structure method CBS-QB3, combined with RRKM/ME rate modeling. The study identifies two primary pathways: (*i*) the addition of SiH_3 to the double bond, and (*ii*) H-abstraction by SiH_3, resulting in various products. The addition pathway produces two major products, **P3** and **P4**, while the H-abstraction pathway generates **P1** + SiH_4 and **P2** + SiH_4. Among these, the adduct **P3** is determined to be the most thermodynamically and kinetically favorable intermediate (T < 900 K). However, at very high temperatures (T > 900 K), **P1** and **P4** gain prominence. Pressure effect analysis (at

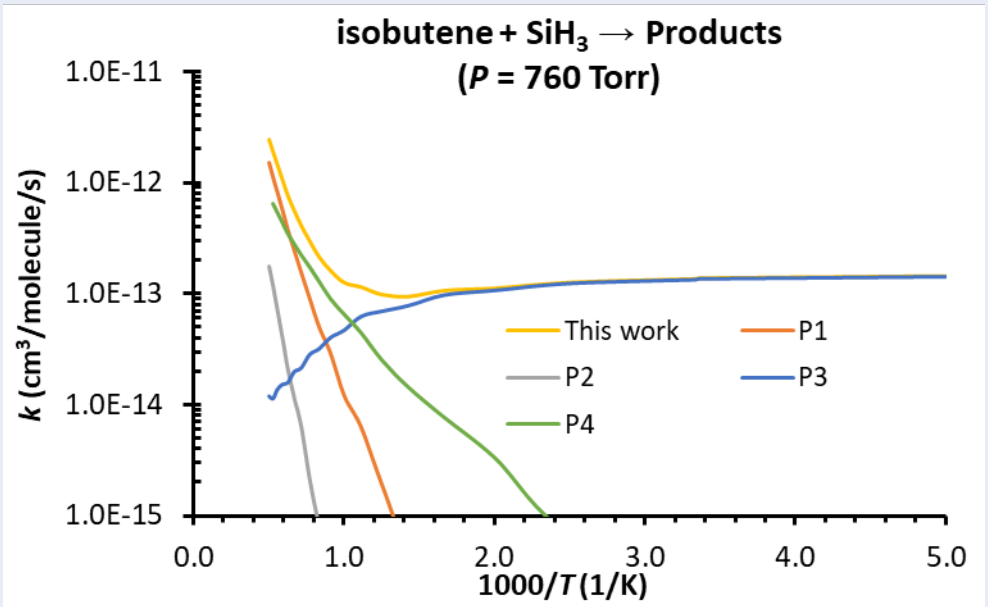

Figure 4: Calculated total and individual k(T, P) for the isobutene + SiH_3 → products reaction

Table 2: Branching ratio for the isobutene + SiH_3 → products reaction.

T (K)	RC	P1	P2	P3	P4
200	0.1	0.1	0.1	99.8	0.1
298	0.1	0.1	0.1	99.7	0.2
300	0.1	0.1	0.1	99.4	0.4
400	0.1	0.1	0.1	99.2	0.6
500	0.1	0.1	0.1	96.8	3.0
600	0.1	0.2	0.1	92.4	7.3
700	0.1	0.5	0.1	84.0	15.4
800	0.1	2.0	0.1	71.7	26.1
900	0.1	5.6	0.1	55.0	39.3
1000	0.1	9.7	0.1	37.8	52.4
1100	0.0	18.2	0.1	25.3	56.3
1200	0.0	23.6	0.4	15.1	60.9
1300	0.0	30.7	0.7	9.6	59.0
1400	0.0	37.9	1.5	5.3	55.2
1500	0.0	44.1	2.1	3.5	50.3
1600	0.0	49.4	2.7	2.1	45.8
1700	0.0	53.5	3.8	1.4	41.2
1800	0.0	56.7	4.9	1.0	37.5
1900	0.0	59.0	6.1	0.6	34.3
2000	0.0	61.9	7.1	0.5	30.5

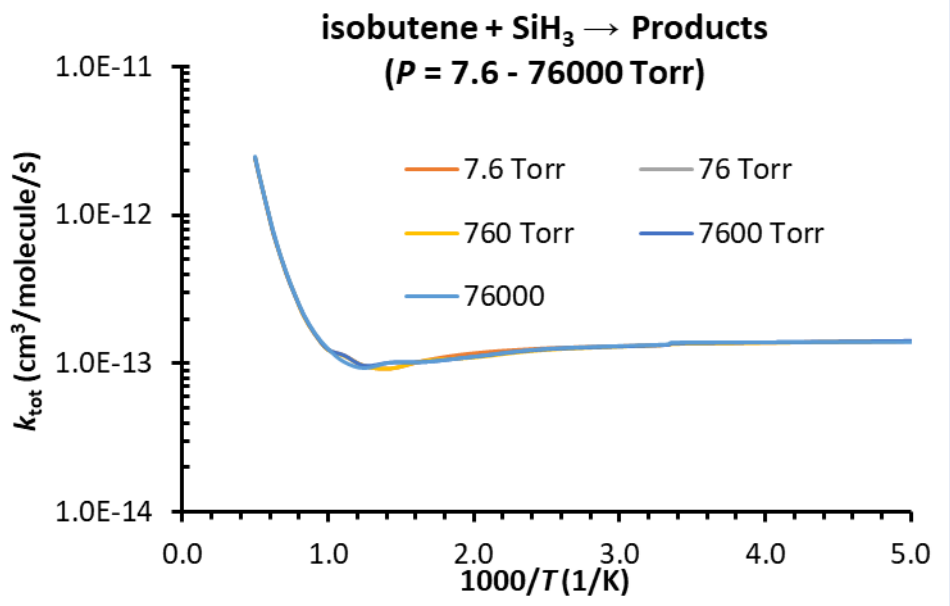

Figure 5: Pressure effect analysis for the isobutene + SiH_3 → products reaction.

P = 7.6 - 76000 Torr) confirms that pressure has no significant influence on the reaction mechanism. The barrierless formation of RC plays a minor role in the hydrosilylation process, resulting in only a 1.0 to 1.7-fold difference in the total rate constant. The branching ratio for product formation in the reaction confirms quantitatively that **P3** is dominant at temperatures below 900 K, reaching a maximum of 99.8% at 200 K. At higher temperatures, **P1** and **P4** become dominant, with branching ratios of 61.9% and 30.5%, respectively, at 2000 K. Thermodynamic properties for isobutene are obtained, revealing the atomization scheme at the CBS-QB3 level is suitable for S^{298K} and $C_p{}^{298K}$, while the isodesmic reaction scheme is recommended for $\triangle_f H^{298K}$ calculations. The calculated geometrical parameters, thermodynamic properties, and kinetic data align with existing/related literature, indicating the reliability of the study. These findings provide a robust basis for detailed kinetic modeling of silicon CVD processes, which are of substantial technological importance.

ABBREVIATIONS

B3LYP: Becke, 3-parameter, Lee-Yang-Parr
CVD: Chemical vapor deposition
CBS-QB3: Complete basis set - Quadratic Becke3
HIR: Hindered internal rotation
IRC: Intrinsic reaction coordinate
ILT: Inverse Laplace transform
MEP: Minimum energy paths
MSMC: Multi-Species Multi-Channels
PECVD: Plasma-enhanced chemical vapor deposition
P: Products
RRKM-ME: Rice–Ramsperger–Kassel–Marcus based master equation
TSs: Transition states.

CONFLICT OF INTERESTS

The authors declare that they have no competing interests.

AUTHORS' CONTRIBUTIONS

Uyen N-P. Tran: Data curation, Visualization, Investigation, Writing – original draft. Loc T. Nguyen: Data curation, Formal analysis, Investigation, Validation, Visualization, Writing – original draft. Tam V.-T. Mai: Conceptualization, Data curation, Formal analysis, Methodology, Validation, Visualization, Writing – review & editing. Khoi M. Le: Data curation, Formal analysis. Lam K. Huynh: Conceptualization, Funding acquisition, Methodology, Resources, Software, Supervision, Writing – review & editing.

FUNDING

This research is funded by Vietnam National University HoChiMinh City (VNU-HCM) under grant number 562-2023-28-01.

AVAILABILITY OF DATA AND MATERIALS

Data will be made available on request.

ETHICS APPROVAL AND CONSENT TO PARTICIPATE

Not applicable.

CONSENT FOR PUBLICATION

Not applicable.

COMPETING INTERESTS

The author(s) declare that they have no competing interests.

ACKNOWLEDGEMENTS

This research is funded by Vietnam National University Ho Chi Minh City under grant number 562-2023-28-01. We would like to thank Tri Pham (Institute for Computational Science and Technology at Ho Chi Minh City) for their technical assistance.

REFERENCES

1. and Li J TZ, Y Y. Theoretical ab-initio kinetics of the reactions between isobutene plus hydroxyl. Chem Phys Lett. 2019;720:83–92.
2. SE S. Silicon Carbide Technology for Advanced Human Healthcare Applications. Micromachines. 2022;13(3). Available from: https://doi.org/10.3390/mi13030346.
3. P M. Silicon carbide and silicon carbide-based structures. Surf Sci Rep. 2002;48(1-4):1–51.
4. EA F, D H, SD E. Understanding the Mechanism of SiC Plasma-Enhanced Chemical Vapor Deposition (PECVD) and Developing Routes toward SiC Atomic Layer Deposition (ALD) with Density Functional Theory. ACS Appl Mater Interfaces. 2018;10(17):15216–15225.
5. A M, K T. Investigation of the growth kinetics of glow-discharge hydrogenated amorphous silicon using a radical separation technique. J Appl Phys. 1986;60(7):2351–2356.
6. A M. Thin-Film Silicon –Growth Process and Solar Cell Application. Jpn J Appl Phys. 2004;43(12):7909–7920.
7. Y N, S S. Hydrosilylation reaction of olefins: recent advances and perspectives. RSC Adv. 2015;5(26):20603–20616.
8. SK L, DB B, JM J. Absolute rate constants for the reaction of silyl with nitric oxide, ethylene, propyne, and propylene, and the silyl recombination reaction. Chem Phys Lett. 1990;169(1-2):55–63.
9. SK L, JM J. Direct kinetic studies of SiH3+SiH3, H, CCl4, SiD4, Si2H6, and C3H6 by tunable infrared diode laser spectroscopy. J Chem Phys. 1991;95(7):4914–4926.
10. A B. Theoretical Study of the Reaction of Silyl Radical with Ethylene and Propylene. J Phys Chem A. 1997;101(24):4402–4408.
11. C C, KU I, JC S. Absolute rate constants for the addition of triethylsilyl radicals to various unsaturated compounds. J Am Chem Soc. 2002;105(10):3292–3296.
12. OJ C, GA D. Theoretical study of the thermochemistry and kinetics of the addition of silyl radical to ethylene. Chem Phys Lett. 2006;425(4-6):201–204.
13. Y L, and Suo Y WZ. Theoretical study on the mechanism for the addition reaction of SiH(3) with propylene and acetic acid. J Phys Chem A. 2006;110(45):12439–12442.
14. MJ F, GW T, HB S, GE S, MA R, JR C, et al. Gaussian 16. Wallingford CT: Gaussian, Inc. 2009;.
15. JA M, MJ F, JW O, GA P. A complete basis set model chemistry. VI. Use of density functional geometries and frequencies. J Chem Phys. 1999;110(6):2822–2827.
16. C L, and Parr RG YW. Development of the Colle-Salvetti correlation-energy formula into a functional of the electron density. Phys Rev B. 1988;37(2):785–789.
17. AD B. Density-functional exchange-energy approximation with correct asymptotic behavio. Phys Rev A. 1998;38(6):3098–3100.
18. PJ S, FJ D, CF C, MJ F. Ab initio calculation of vibrational absorption and circular dichroism spectra using density functional force fields. J Phys Chem. 1994;98(45):11623–11627.
19. J P, M S, M D, J R. Analysis of the effect of changing the a0 parameter of the Becke3-LYP hybrid functional on the transition state geometries and energy barriers in a series of prototypical reactions. Phys Chem Chem Phys. 2002;4(5):722–731.
20. TH D. Gaussian basis sets for use in correlated molecular calculations. I. The atoms boron through neon and hydrogen. J Chem Phys. 1989;90(2):1007–1023.
21. H T, KC L. Pathways, kinetics and thermochemistry of methyl-ester peroxy radical decomposition in the low-temperature oxidation of methyl butanoate: A computational study of a biodiesel fuel surrogate Combust Flame. Combust Flame. 2014;161(9):2270–2287.
22. C G, HB S. An improved algorithm for reaction path following. J Chem Phys. 1989;90(4):2154–2161.
23. C G, HB S. Reaction path following in mass-weighted internal coordinates. J Phys Chem. 1990;94(14):5523–5527.
24. M S, M-F R, GB M, Van Speybroeck V, M W. Ab Initio Calculations for Hydrocarbons: Enthalpy of Formation, Transition State Geometry, and Activation Energy for Radical Reactions. J Phys Chem A. 2003;107(43):9147–9159.
25. DA M. Statistical mechanics: Sterling Publishing Company; 2000.
26. MV D, HT N, N T, TNM L, LK H. Multi-Species Multi-Channel (MSMC): An Ab Initio-based Parallel Thermodynamic and Kinetic Code for Complex Chemical Systems. Int J Chem Kinet. 2015;47(9):564–575.
27. DT G. A general method for numerically simulating the stochastic time evolution of coupled chemical reactions. J Comput Phys. 1976;22(4):403–434.
28. DT G, A H, LR P. Perspective: Stochastic algorithms for chemical kinetics. J Chem Phys. 2013;138(17):170901.
29. JA M, SJ K. Master equation methods in gas phase chemical kinetics. J Phys Chem A. 2006;110(36):;110(36):10528–10544.
30. MV D, HT N, TV M, LK H. Global minimum profile error (GMPE) - a least-squares-based approach for extracting macroscopic rate coefficients for complex gas-phase chemical reactions. Phys Chem Chem Phys. 2018;20(2):1231–1239.
31. C E. The Penetration of a Potential Barrier by Electrons. Phys Rev. 1930;35(11):1303–1309.
32. TV M, TT N, HT N, LK H. New Mechanistic Insights into Atmospheric Oxidation of Aniline Initiated by OH Radicals. Environ Sci Technol. 2021;55(12):7858–7868.
33. H H, J T, HJ W. Collisional deactivation of vibrationally highly excited polyatomic molecules. II. Direct observations for excited toluene. J Chem Phys . 1983;78(11):6709–6717.
34. BE P, JM P, JP O. The properties of gases and liquids: Mcgraw-hill New York; 2001.
35. T B, DF S. Algorithm 448: number of multiply-restricted partitions. Commun ACM. 1973;16(6).
36. JW C, JW T. An Algorithm for the Machine Calculation of Complex Fourier Series. Math Comput . 1965;19(90):297–301.
37. SH R, MJ P, DL B, NJB G. Fitting of pressure-dependent kinetic rate data by master equation/inverse Laplace transform analysis. J Phys Chem. 1995;99(36):13452–13460.
38. Y G, SJ K. Long-range transition state theory. J Chem Phys. 2005;122(19):194103.
39. TVT M, Mv D, LK H. Theoretical kinetics of the C2H4 + NH2 reaction. . Combust Flame. 2020;215:193–202.

40. C Y, E H. Detection of the silyl radical SiH3 by infrared diode-laser spectroscopy. Phys Rev Lett. 1986;56(9):923–925.
41. K K. Structure of free polyatomic molecules: basic data: Springer Science & Business Media; 2013.
42. TH H, MLaLK. RGA4HoF. Reaction Generator and Analyzer for Accurate Heat of Formation Calculation for Chemical Species. 2021;.
43. B R, RE P, Gv L, D K, A B, D L, et al. Active Thermochemical Tables: thermochemistry for the 21st century. J Phys Conf Ser. 2005;16:561–570.
44. EJ P, FW M, FD R. Heats of combustion, formation, and isomerization of ten C4 hydrocarbons. J Res Natl Bur Stand. 1951;46(2).
45. DR S, EF W, GC S. The chemical thermodynamics of organic compounds; 1969.
46. FD R. Selected values of chemical thermodynamic properties: US Government Printing Office; 1952.